Letter | Editors' Suggestion

Crucial role of thermal fluctuations and vertex corrections for the magnetic pseudogap

Mengxing Ye [1,2] and Andrey V. Chubukov [3]

[1] *Kavli Institute for Theoretical Physics, University of California, Santa Barbara, California 93106, USA*
[2] *Department of Physics and Astronomy, University of Utah, Salt Lake City, Utah 84112, USA*
[3] *School of Physics and Astronomy and William I. Fine Theoretical Physics Institute, University of Minnesota, Minneapolis, Minnesota 55455, USA*

(Received 12 June 2023; accepted 26 July 2023; published 22 August 2023)

It is generally believed that in a two-dimensional metal, whose ground state is antiferromagnetically ordered with $\mathbf{Q} = (\pi, \pi)$, thermal (static) magnetic fluctuations give rise to precursor behavior above T_N in which the spectral function of a hot fermion (the one for which $\mathbf{k}$ and $\mathbf{k} + \mathbf{Q}$ are Fermi surface points) contains two peaks, separated by roughly the same energy as in the antiferromagnetically ordered state. The two peaks persist in some range of $T > T_N$ and eventually merge into a single peak at zero frequency. This behavior is obtained theoretically by departing from free fermions in a paramagnet and evaluating the dressed fermionic Green's function by summing up infinite series of diagrams with contributions from thermal magnetic fluctuations. We show, following [Y. M. Vilk and A.-M. S. Tremblay, J. Phys. I (France) **7**, 1309 (1997)] that keeping vertex renormalization diagrams in these series is crucial as other terms only broaden the spectral function of a hot fermion but do not shift its maximum away from zero frequency. As the consequence, the magnetic pseudogap should be treated as an input for theories that neglect vertex corrections, such as, e.g., Eliashberg theory for magnetically mediated superconductivity. We also analyze the potential pseudogap behavior at $T = 0$. We argue that it may exist, but only at a finite correlation length, and not as a precursor to antiferromagnetism.

DOI: 10.1103/PhysRevB.108.L081118

Introduction. The origin of the pseudogap behavior, observed in the cuprates and other correlated materials remains the subject of ongoing debate. Theoretical proposals for the pseudogap can be broadly split into three categories. One identifies pseudogap behavior with some particle-hole order either a conventional one, such as a charge-density wave [1–5], or less conventional, such as a circulating current [6,7]. Another identifies the pseudogap with a spin-liquid-type "mother" state from which one gets antiferromagnetism, superconductivity, and charge order [8–12]. And the third treats the pseudogap phase as a precursor to an ordered state—either a spin-density-wave (SDW) order [13–30], superconductivity [20,31–37], or pair-density wave [38].

In this Letter, we focus on the last category and discuss some aspects of a precursor to an SDW order with $\mathbf{Q} = (\pi, \pi)$ in two dimensions. We analyze the emergence of peaks at a finite frequency in the spectral function of a fermion on the Fermi surface, particularly, at a hot spot $\mathbf{k}_{\rm hs}$ for which $\mathbf{k}_{\rm hs}$ and $\mathbf{k}_{\rm hs} + \mathbf{Q}$ are both on the Fermi surface. The emergence of such peaks without a full gap between them is a signature feature of pseudogap behavior.

We address two issues. The first is about pseudogap behavior caused by thermal magnetic fluctuations [14,16–20,22,23,25–28,30]. Several groups, including us, demonstrated [16,17,19,20,22,25,30] that that pseudogap does develop when one includes infinite series of contributions to the fermionic Green's function from thermal (static) spin fluctuations. In this Letter, we look more closely at the interplay between noncrossed and crossed diagrams in these series. The noncrossed diagrams renormalize the Green's function of an intermediate fermion $G_0(\mathbf{k} + \mathbf{q}, \omega_m) \to G(\mathbf{k} + \mathbf{q}, \omega_m)$ and can be absorbed into the self-consistent one-loop theory (SCOLT). The crossed diagrams describe vertex corrections. Previous studies [13,14,18,26] found that at large dimensionless spin-fermion coupling $\lambda_{\rm th}$, the noncrossed diagrams, taken alone, broaden the spectral function of a hot fermion, but the maximum remains at $\omega = 0$, i.e., pseudogap does not emerge. Here, we show that (i) pseudogap behavior does not develop within SCOLT for any value of $\lambda_{\rm th}$, (ii) SCOLT is the "boundary" case in the sense that already infinitesimally small vertex corrections give rise to a pseudogap, and (iii) SCOLT is a member of a one-parameter set of such boundary models, which do not display pseudogap behavior, but develop it upon an infinitesimally small perturbation.

Second, we analyze whether the system can potentially display pseudogap behavior at $T = 0$. We argue that this holds in the weak-coupling regime away from the SDW quantum-critical point (QCP) when SDW fluctuations are gapped and weakly damped. Close to the SDW QCP, Landau damping takes over, and $A(\mathbf{k}_{\rm hs}, \omega)$ has a maximum at $\omega = 0$. This agrees with the recent study by Grossman and Berg [39]. In a generic case when fermionic velocity v_F and bosonic velocity v_s are comparable, pseudogap behavior ends up when the system enters the strong-coupling regime near a QCP. If, however, v_s is small compared to v_F, pseudogap behavior extends into the strong-coupling regime. We emphasize that this pseudogap is not a precursor to SDW as the magnitude of the pseudogap in $A(\mathbf{k}_{\rm hs}, \omega)$ is set by the mass of the SDW fluctuations, and it must disappear before a QCP.

Pseudogap due to thermal fluctuations. We consider a system of fermions, interacting by exchanging spin fluctuations with momentum near $\mathbf{Q}$. We take as an input that static spin

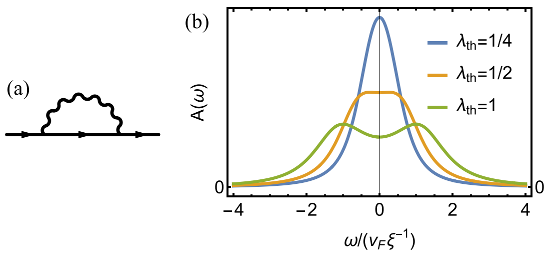

FIG. 1. (a) One-loop self-energy. (b) Spectral function at the hot spot from the one-loop calculation. As the dimensionless coupling $\lambda_{\text{th}} = \frac{3\bar{g}T}{2\pi(v_F\xi^{-1})^2}$ increases, the spectral function shows pseudogap behavior when $\lambda_{\text{th}} > \lambda_c = 0.47$.

fluctuations have the Ornstein-Zernike form with a large but finite correlation length $\xi = \xi(T)$ and are coupled to fermions by Yukawa coupling $\bar{g}$, which we assume to be comparable to the bandwidth. Our goal is to obtain the spectral function $A(\mathbf{k}_{\text{hs}}, \omega) = -(1/\pi)\ \text{Im}\, G_{\text{ret}}(\mathbf{k}_{\text{hs}}, \omega)$ for a hot fermion and verify whether at a finite T and large, but still finite ξ, its maximum splits into two maxima at a finite frequency, and whether vertex corrections are crucial for the spitting. For this specific goal, it is sufficient to treat $\xi = \xi(T)$ as an input parameter (for self-consistent calculations of $\xi(T)$ see Refs. [21,30]).

The spectral function generally can easily obtained by evaluating the thermal self-energy $\Sigma_{\text{th}}(\mathbf{k}_{\text{hs}}, \omega)$. We first compute it at the one-loop order, use the result to rationalize the need to include higher-loop contributions, and then analyze $A(\mathbf{k}_{\text{hs}}, \omega)$ and the dressed $\Sigma_{\text{th}}(\mathbf{k}_{\text{hs}}, \omega)$ with and without vertex corrections.

The one-loop thermal self-energy, shown in Fig. 1(a), is the convolution of a propagator of a free fermion, $G^{(0)}(\mathbf{k}_{\text{hs}} + \mathbf{Q} + \mathbf{q}, \omega)$ and a static spin propagator $\chi(\mathbf{q}) = 1/(\mathbf{q}^2 + \xi^{-2})$. Expanding the fermionic dispersion to linear order in $\mathbf{q}$ and integrating over the two components of $\mathbf{q}$, one obtains the exact analytical expression [14,18,21,26,30],

$$\Sigma^{(1)}_{\text{th}}(\mathbf{k}_{\text{hs}}, \omega) = v_F\xi^{-1}\lambda_{\text{th}}\left[\text{sgn}(\mathsf{w})\frac{\ln[\mathsf{w} + \sqrt{(\mathsf{w})^2 + 1}]}{\sqrt{(\mathsf{w})^2 + 1}} - i\frac{\pi}{2\sqrt{(\mathsf{w})^2 + 1}}\right], \tag{1}$$

where $\lambda_{\text{th}} = \{3\bar{g}T(2\pi(v_F\xi^{-1})^2]\}$ is the dimensionless "thermal" coupling, and $\mathsf{w} = \omega/(v_F\xi^{-1})$ is the dimensionless frequency. The dimensionless coupling grows as the system approaches the onset temperature T_N of the (π, π) order.

We show the spectral function $A^{(1)}(\mathbf{k}_{\text{hs}}, \mathsf{w}) = -(1/\pi)\ \text{Im}\{[v_F\xi^{-1}\mathsf{w} - \Sigma^{(1)}_{\text{th}}(\mathbf{k}_{\text{hs}}, \mathsf{w})]^{-1}\}$ in Fig. 1(b). At small λ_{th}, $A^{(1)}(\mathbf{k}_{\text{hs}}, \mathsf{w})$ is peaked at $\mathsf{w} = 0$ as is expected for a weakly interacting fermion at the Fermi surface. However, once λ_{th} exceeds the critical value of $\lambda_c = 2\sqrt{2}/(2\sqrt{2} + \pi) \approx 0.4738$, the maximum of $A^{(1)}(\mathbf{k}_{\text{hs}}, \mathsf{w})$ shifts to a fiRnite $|\mathsf{w}| = \tilde{\Delta}_{\text{pg}} \sim \sqrt{\lambda - \lambda_c}$. The pseudogap behavior becomes particularly pronounced at large λ_{th}, where $\tilde{\Delta}_{\text{pg}} > v_F\xi^{-1}$, and at $\omega \sim \tilde{\Delta}_{\text{pg}}$,

$$\int_{\mathbf{q}} G^{(0)}(\mathbf{k}_{\text{hs}} + \mathbf{Q} + \mathbf{q}, \omega)\chi(\mathbf{q}) \approx G^{(0)}(\mathbf{k}_{\text{hs}} + \mathbf{Q}, \omega)\int_{\mathbf{q}} \chi(\mathbf{q}), \tag{2}$$

such that $\Sigma^{(1)}_{\text{th}}(\mathbf{k}_{\text{hs}}, \omega) \approx \tilde{\Delta}^2_{\text{pg}}/\omega$ [14,18,21,26,30] with $\tilde{\Delta}_{\text{pg}} = (v_F\xi^{-1})(\lambda\ \ln\lambda)^{1/2}/\sqrt{2} \approx (\frac{3\bar{g}T}{2\pi}\ln\xi)^{1/2}$. Here, $\int_{\mathbf{q}} = \int d^2\mathbf{q}$. This self-energy is the same as in the SDW-ordered state, hence, the emergence of the peaks at $|\omega| = \tilde{\Delta}_{\text{pg}}$ is quite natural [below the peak, $\text{Im}\,\Sigma^{(1)}(\mathbf{k}_{\text{hs}}, \omega)$ remains nonzero down to the lowest frequencies, hence, $\tilde{\Delta}_{\text{pg}}$ is a pseudogap rather than a true gap].

We see that the pseudogap behavior does emerge within the one-loop approximation, however, the coupling λ_{th} must exceed $\lambda_c = O(1)$. This raises the question whether the one-loop result stands once we include higher-order terms. Examples of higher-order diagrams for $\Sigma(\mathbf{k}_{\text{hs}}, \omega)$ are shown in Fig. 2. They include noncrossed diagrams [Fig. 2(a)], which account for the renormalization of the internal fermionic line, and crossed diagrams [Fig. 2(b)], which represent vertex corrections. Besides, the chemical potential μ is different from $\mu_0 = \epsilon_{\mathbf{k}_{\text{hs}}}$ and is obtained self-consistently from the condition on the fermionic density. Below, we incorporate the change in the chemical potential into $\omega \to \bar{\omega} = \omega + \delta\mu$, where $\delta\mu = \mu - \epsilon_{\mathbf{k}_{\text{hs}}} = \mu - \mu_0$.

As a first step, let us keep only noncrossed higher-loop diagrams, i.e., neglect vertex corrections. The fully dressed self-energy is given by the same one-loop diagram as in the perturbation theory but with the fully dressed propagator of an intermediate fermion. This is the SCOLT. The retarded Green's function is $G^{\text{sc}}(\mathbf{k}_{\text{hs}}, \bar{\mathsf{w}})^{-1} = v_F\xi^{-1}X$ (sc stands for self-consistent), where $\bar{\mathsf{w}} = \bar{\omega}/v_F\xi^{-1}$, and $X = X(\bar{\mathsf{w}})$ is the solution of

$$X = \bar{\mathsf{w}} - \lambda_{\text{th}}\frac{\ln(X + \sqrt{X^2 + 1})}{\sqrt{X^2 + 1}} + i\lambda_{\text{th}}\frac{\pi}{2\sqrt{X^2 + 1}}. \tag{3}$$

Expanding at small $\bar{\mathsf{w}}$, we find [see the Supplemental Material (SM) in Ref. [40] for details], $X = a\bar{\mathsf{w}} + ib(1 - c\bar{\mathsf{w}}^2) + \cdots$, where a b, and c are functions of λ_{th}, and the dots stand for terms of higher order in $\bar{\mathsf{w}}$. The spectral function $A(\mathbf{k}_{\text{hs}}, \bar{\mathsf{w}}) \propto 1/[b^2 + \bar{\mathsf{w}}^2(a^2 - b^2c)]$. The pseudogap emerges when the prefactor for $\bar{\mathsf{w}}^2$ is negative, i.e., when $a^2 < b^2c$. We expanded analytically in $\bar{\mathsf{w}}^2$ and found that this does not happen at any value of λ_{th}: the quasiparticle peak broadens as λ_{th} increases, but remains centered at $\omega = 0$. At large λ_{th}, when $\tilde{\Delta}_{\text{pg}} > v_F\xi^{-1}$, the spectral function has a semicircular form $A^{\text{sc}}(\mathbf{k}_{\text{hs}}, \bar{\omega}) = \sqrt{4\tilde{\Delta}^2_{\text{pg}} - \bar{\omega}^2}/(2\pi\tilde{\Delta}^2_{\text{pg}})$ at $2\tilde{\Delta}_{\text{pg}} > \bar{\omega} > v_F\xi^{-1}$ [14] and remains smooth at $\omega < v_F\xi^{-1}$ as we verified. This

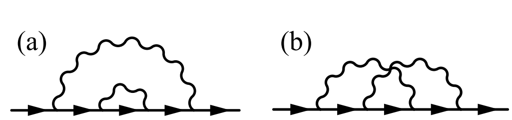

FIG. 2. Noncrossed (a) and crossed (b) two-loop irreducible diagrams.

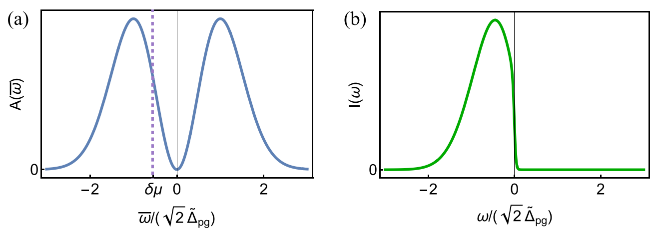

FIG. 3. (a) Spectral function $A^{\rm full}(\mathbf{k}_{\rm hs},\bar\omega)$ and (b) spectral intensity $I^{\rm full}(\mathbf{k}_{\rm hs},\omega)$ for the SU(2) symmetric model [see Eqs. (7)]. The horizontal axis is $\bar\omega=\omega+\delta\mu$ in (a) and ω in (b), both in units of $\sqrt{2}\tilde\Delta_{\rm pg}$.

spectral function describes incoherent excitations extending up to $2\tilde\Delta_{\rm pg}$, and its maximum remains at $\omega=0$ [41].

We next include the crossed diagrams. We compute the full self-energy directly, by extending perturbation theory to infinite order [42]. The computations again simplify at large $\lambda_{\rm th}$ where we can use Eq. (2). Using it for all diagrams, we find that at each loop order, the crossed and the noncrossed diagrams are of the same order, and each set forms a series in $G^{(0)}(\mathbf{k}_{\rm hs}+\mathbf{Q},\bar\omega)G^{(0)}(\mathbf{k}_{\rm hs},\bar\omega)\tilde\Delta^2_{\rm pg}$. This allows one to keep only one diagram at a given loop order m and multiply it by the proper combinatoric factor $\mathcal{D}_m$. For the SU(2)-symmetric problem, $\mathcal{D}_m=(2m+1)!!$ [16,22]. The full Green's function is then $G^{\rm full}(\mathbf{k}_{\rm hs},\bar\omega)=G^{(0)}(\mathbf{k}_{\rm hs},\bar\omega)C(\bar\omega)$, where

$$C(\bar\omega)=\sum_m(2m+1)!!\big[\tilde\Delta^2_{\rm pg}G^{(0)}(\mathbf{k}_{\rm hs},\bar\omega)G^{(0)}(\mathbf{k}_{\rm hs}+\mathbf{Q},\bar\omega)\big]^m. \tag{4}$$

Reexpressing the infinite sum as the integral,

$$C(\bar\omega)=\frac{2}{\sqrt{\pi}}\int_0^\infty dt\, e^{-t}\frac{t^{1/2}}{1-ut}, \tag{5}$$

where $u=2\tilde\Delta^2_{\rm pg}G^{(0)}(\mathbf{k}_{\rm hs},\bar\omega)G^{(0)}(\mathbf{k}_{\rm hs}+\mathbf{Q},\bar\omega)$ and evaluating it, we obtain for a fermion at a hot spot,

$$C(\bar\omega)=\mathsf{C}(z)=2z^2\{[\sqrt{\pi}ze^{-z^2}{\rm Erfi}(z)-1]-i\sqrt{\pi}ze^{-z^2}\}, \tag{6}$$

where $z=\bar\omega/(\tilde\Delta_{\rm pg}\sqrt{2})$ and Erfi(z) is the imaginary error function. The spectral function is

$$A^{\rm full}(\mathbf{k}_{\rm hs},\bar\omega)=\frac{1}{\sqrt{2\pi}\,\tilde\Delta_{\rm pg}}\frac{\bar\omega^2}{\tilde\Delta^2_{\rm pg}}\exp\left[-\frac{\bar\omega^2}{2\tilde\Delta^2_{\rm pg}}\right]. \tag{7}$$

We plot the full spectral function in Fig. 3(a). We see that it does display the pseudogap behavior. The form of the full $A^{\rm full}(\mathbf{k}_{\rm hs},\bar\omega)$ is rather similar to the one-loop result at $\lambda_{\rm th}\gg 1$, and the value of the full pseudogap $\Delta_{\rm pg}$ is comparable to $\tilde\Delta_{\rm pg}$[43].

A complimentary way to understand the importance of vertex corrections is to analyze the structure of the thermal self-energy. The Dyson equation expresses it in terms of the full Green's function $G^{\rm full}(\mathbf{k}_{\rm hs}+\mathbf{Q},\bar\omega)$ and the full vertex $\Gamma(\mathbf{k}_{\rm hs},\bar\omega)$ as

$$\Sigma_{\rm th}(\mathbf{k}_{\rm hs},\bar\omega)=3\tilde\Delta^2_{\rm pg}G^{\rm full}(\mathbf{k}_{\rm hs}+\mathbf{Q},\bar\omega)\Gamma(\mathbf{k}_{\rm hs},\bar\omega). \tag{8}$$

In the SCOLT, $\Gamma(\mathbf{k}_{\rm hs},\bar\omega)=1$. Using $G^{\rm full}=(G^{(0)}-\Sigma)^{-1}$, we find

$$\Sigma_{\rm th}(\mathbf{k}_{\rm hs},\bar\omega)=\sqrt{2}\tilde\Delta_{\rm pg}\bar\Sigma(z),\quad \bar\Sigma(z)=\frac{z[\mathsf{C}(z)-1]}{\mathsf{C}(z)}$$
$$\Gamma(\mathbf{k}_{\rm hs},\bar\omega)=\Gamma(z)=\frac{2}{3}z^2\frac{\mathsf{C}(z)-1}{\mathsf{C}^2(z)}. \tag{9}$$

Because $\mathsf{C}(z)$ is complex, $\bar\Sigma(z)$ and $\Gamma(z)$ are complex functions of the frequency. The spectral function is $A^{\rm full}(\mathbf{k}_{\rm hs},\bar\omega)=A^{\rm full}(z)$, where

$$A^{\rm full}(z)=\left(-\frac{1}{\pi\sqrt{2}\tilde\Delta_{\rm pg}}\right)\frac{{\rm Im}\,\bar\Sigma(z)}{[z-{\rm Re}\,\bar\Sigma(z)]^2+[{\rm Im}\,\bar\Sigma(z)]^2}. \tag{10}$$

We plot real and imaginary parts of $\bar\Sigma(z)$ and $\Gamma(z)$ in Figs. 4(a) and 4(b). We see that Im $\bar\Sigma(z)$ is a rather smooth function of z and is featureless around $z=1$ where the spectral function has a pseudogap peak [see Fig. 3(a)]. On more careful look, we find that the peak in $A^{\rm full}(z)$ at $z=1$ emerges because Re $\bar\Sigma(z)-z$ changes sign very near $z=1$ [see Fig. 4(a)]. Furthermore, Re $\bar\Sigma(z)=\{3/(2z)[{\rm Re}\,\mathsf{C}(z){\rm Re}\,\Gamma(z)-{\rm Im}\,\mathsf{C}(z){\rm Im}\,\Gamma(z)]\}$. We plot the two parts of this expression separately in Fig. 4(c). We see that near $z=1$, Im $\mathsf{C}(z)$Im $\Gamma(z)\gg$ Re $\mathsf{C}(z)$Re $\Gamma(z)$. This implies that the imaginary part of the vertex $\Gamma(z)$ is crucial for the pseudogap. One could not obtain the peak in $A^{\rm full}(z)$ if $\Gamma(z)$ was a constant, such as in the SCOLT.

We note in passing that this analysis is different from the one in Refs. [27,28]. These authors analyzed the vertex function on the Matsubara axis. The latter is complex at a hot spot due to a finite $\delta\mu$, which makes even $G^{(0)}(\mathbf{k}_{\rm hs}.\omega_m)=1/(i\omega_m+\delta\mu)$ complex (Refs. [44–46]). In Fig. 4(d), we plot the real and imaginary parts of $\Gamma(\omega_m)$ for $\delta\mu=0$ (dashed lines) and $\delta\mu=-0.8$ (solid lines) in unit of $\sqrt{2}\tilde\Delta_{\rm pg}$. We see that Im $\Gamma(z_m)$ is finite for $\delta\mu\neq 0$. The behavior of Re $\Gamma(z_m)$, Im $\Gamma(z_m)$ for $\delta\mu=-0.8$ is quite similar to the vertex function extracted from the numerical analysis of the self-energy in Refs. [27,28]. At the same time, our results do not support the key point of Refs. [27,28] that the complex structure of $\Gamma(\omega_m)$ on the Matsubara axis is the key to pseudogap development. Indeed, on the real axis, $\delta\mu$ shifts the frequency ω to $\bar\omega$, but the two-peak pseudogap behavior emerges independent of the value of $\delta\mu$ and would hold even if $\delta\mu$ was zero [47]. A similar behavior of vertex function Γ in real and imaginary frequencies has been observed in Ref. [48] using dynamical mean-field theory.

On a more careful look, we found that not all diagrammatic series with both noncrossed and crossed diagrams lead to pseudogap behavior. An example is the series with the combinatoric factor $\mathcal{D}_m=(2m-1)!!$, which holds in certain one-dimensional models [42] and two-dimensional models on a triangular lattice [25]. These series yield $A^{\rm full}(\mathbf{k}_{\rm hs},\omega)\propto\exp[-\bar\omega^2/(2\tilde\Delta^2_{\rm pg})]$, which is peaked at $\omega=0$. For a generic $\mathcal{D}_m$, the series can be represented as a continued fraction,

$$G^{\rm full}(\mathbf{k}_{\rm hs},i\omega_n)=\cfrac{1}{i\omega_n-\cfrac{\kappa_1\tilde\Delta^2_{\rm pg}}{i\omega_n-\cfrac{\kappa_2\tilde\Delta^2_{\rm pg}}{i\omega_n-\cfrac{\kappa_3\tilde\Delta^2_{\rm pg}}{i\omega_n-\cdots}}}}. \tag{11}$$

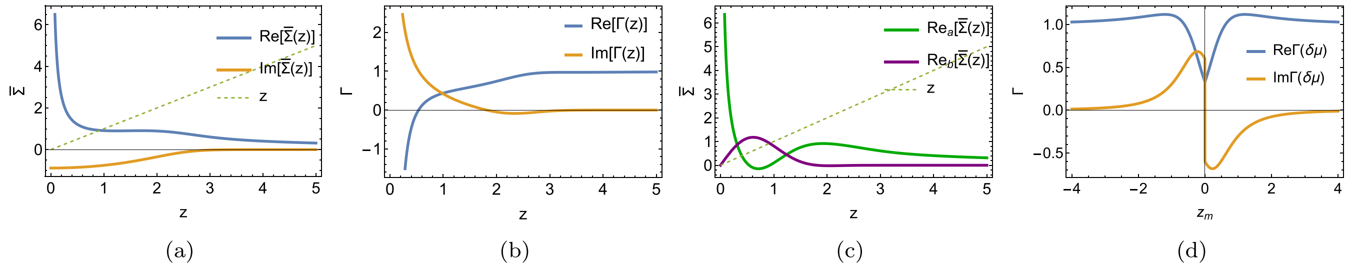

FIG. 4. Panels (a) and (b): real and imaginary parts of the (a) normalized self-energy and (b) the vertex function as functions of $z = (\omega + \delta\mu)/(\tilde{\Delta}_{\rm pg}\sqrt{2})$ from Eq. (9). The spectral function has a peak at $z \approx 1$, where Re $\bar{\Sigma}(z)$ crosses z. Panel (c): two components of Re $\bar{\Sigma}(z)$: Re$_a = (3/2z) = \mathsf{C}(z)$Re $\Gamma(z)$ and Re$_b = -(3/2z)$Im $\mathsf{C}(z)$Im $\Gamma(z)$. Near $z = 1$, Re $\bar{\Sigma}(z) \approx z \approx -(3/2z)$Im $\mathsf{C}(z)$Im $\Gamma(z)$. Panel (d): Re $\Gamma(z_m)$ and Im $\Gamma(z_m)$ along the Matsubara axis at $\delta\mu = -0.8$.

We find that for a set of models with $\kappa_j = \kappa^{(0)} + \kappa^{(1)} j$, the spectral function does not show pseudogap behavior. The SCOLT is a member of this set with $\kappa^{(0)} = 1$ and $\kappa^{(1)} = 0$. The case of $\kappa^{(0)}$=0, $\kappa^{(1)}$=1 corresponds to $\mathcal{D}_m$=$(2m-1)!!$. We verified numerically that for each member of this set, an infinitesimally small deviation $\delta\kappa > 0$ for odd j leads to pseudogap formation (see Fig. 5). For the model with $\kappa_j = \kappa^{(1)} j$ we found analytically,

$$A^{\kappa}(\mathbf{k}_{\rm hs}, \omega) \propto |\omega|^{\delta\kappa/\kappa^{(1)}} e^{-\frac{\omega^2}{2\kappa^{(1)}\tilde{\Delta}^2_{\rm pg}}}. \qquad (12)$$

This spectral function has two peaks at $|\omega| = \sqrt{\delta\kappa}\,\tilde{\Delta}_{\rm pg}$.

That SCOLT is the boundary case for the pseudogap formation can also be seen by analyzing a simple toy model [49,50] in which the self-energy at large λ is given by

$$\Sigma^{\rm toy}(\mathbf{k}_{\rm hs}, \omega) = \tilde{\Delta}^2_{\rm pg}[\alpha G(\mathbf{k}_{\rm hs}, \omega) + (1-\alpha)G^{(0)}(\mathbf{k}_{\rm hs}, \omega)], \qquad (13)$$

where $0 \leqslant \alpha \leqslant 1$. This self-energy interpolates between perturbative one-loop theory at $\alpha = 0$ and SCOLT at $\alpha = 1$. The spectral function $A^{\rm toy}(\mathbf{k}_{\rm hs}, \omega)$ is readily obtained by solving the self-consistent equation for the Green's function $G^{-1}(\mathbf{k}_{\rm hs}, \omega) = \omega - \tilde{\Delta}^2_{\rm pg}[\alpha G(\mathbf{k}_{\rm hs}, \omega) + (1-\alpha)G^{(0)}(\mathbf{k}_{\rm hs}, \omega)]$ [see the SM for details]. For any $\alpha < 1$, the maximum of $A^{\rm toy}(\mathbf{k}_{\rm hs}, \omega)$ is at a finite $|\omega| = \tilde{\Delta}_{\rm pg}(1-\alpha)^{1/2}$, at $\alpha = 1$, it is at $\omega = 0$. We again see that the SCOLT is the boundary case for the pseudogap formation.

Pseudogap from quantum fluctuations. We argued above that thermal spin fluctuations give rise to pseudogap behavior as a precursor to the (π, π) ordered state. We now contrast this behavior with the one at $T = 0$. We neglect superconductivity and analyze whether quantum spin fluctuations can give rise to the pseudogap.

We use the same model as before, but with the dynamical spin propagator $\chi(\mathbf{q}, \Omega_m) = \chi_0/[(\Omega_m/v_s)^2 + (\mathbf{q}-\mathbf{Q})^2 + \xi^{-2} + \gamma|\Omega_m|]$, where v_s is spin velocity and the last term is the Landau damping with $\gamma = (4/\pi \sin\theta)\bar{g}/v_F^2$, where θ is the angle between Fermi velocities at $\mathbf{k}_{\rm hs}$ and $\mathbf{k}_{\rm hs} + \mathbf{Q}$ [51]. We restrict with perturbative one-loop analysis as higher-loop terms at $T = 0$ are at most $O(1)$ relative to the one-loop term [51]. The exact one-loop self-energy can be readily obtained (see the SM for details), and its analysis shows that at small $\lambda_{\rm q} = 3\bar{g}/(4\pi v_F \xi^{-1})$, the spectral function $A^{\rm q}(\mathbf{k}_{\rm hs}, \omega)$ nearly vanishes at $|\omega| < v_s\xi^{-1}$ and has a peak at $|\omega| \geqslant v_s\xi^{-1}$. In the opposite limit of large $\lambda_{\rm q}$, the Landau damping term is the strongest one in the spin propagator, and $A^{\rm q}(\mathbf{k}_{\rm hs}, \omega)$ has a broad peak centered at $\omega = 0$. In both cases, the spectral function also has a δ-functional peak at $\omega = 0$ with overall intensity proportional to the quasiparticle residue [39,52]. We analyzed the evolution of the spectral function with increasing $\lambda_{\rm q}$ at various $\alpha_v = v_F/v_s$ and found self-consistently critical $\lambda_{\rm q}^{cr}$, at which pseudogap behavior at $T = 0$ disappears. We show the results in Fig. 6. For generic $\alpha_v = O(1)$,

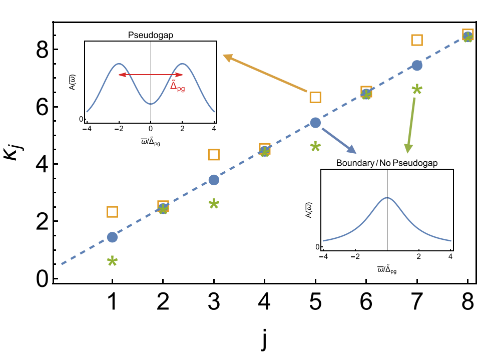

FIG. 5. Ilustration that the set of models with $\kappa_j = \kappa^{(0)} + \kappa^{(1)} j$ [see Eq. (11)] are at the boundary of the pseudogap formaton. The boundary models from the set are along the solid line. We verified that the pseudogap emerges at infinitesimally small $\delta k > 0$ at odd j (orange square).

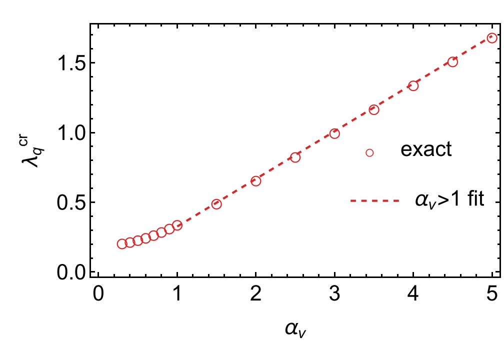

FIG. 6. Critical $\lambda_{\rm q}$ at different $\alpha_v = v_F/v_s$ and $\theta = \pi/2$, i.e., $\gamma = 4\bar{g}/(\pi v_F^2)$. The spectral function shows pseudogap behavior for $\lambda_{\rm q} < \lambda_{\rm q}^{cr}$. Red circles are $\lambda_{\rm q}^{cr}$, extracted from the exact formula for the one-loop self-energy, and dashed line in the linear fit by $\lambda_{\rm q}^{cr} = 0.085 + \mathsf{c}\alpha_v$ with the same prefactor for α_v that we obtained analytically in the $\alpha_v \gg 1$ limit (see the text).

$\lambda_q^{cr} = O(1)$, i.e., there is no pseudogap in the strong-coupling regime. The situation changes when $v_s \ll v_F$, i.e., α_v is large. In this limit, we find analytically $\lambda_q^{cr} = \mathtt{c}\,\alpha_v$, where $\mathtt{c} \approx (3 \sin\theta/16)\sqrt{10/3}$. Still, at large enough ξ, $\lambda_q > \lambda_q^{cr}$, which implies that, near a QCP, the one-loop spectral function does not display pseudogap behavior at $T = 0$. In other words, pseudogap behavior at $T = 0$ is *not* a precursor to SDW [53].

Summary. Previous works have found that in a metal, whose ground state is antiferromagnetically ordered with $\mathbf{Q} = (\pi, \pi)$ thermal magnetic fluctuations give rise to pseudogap behavior in some temperature range above T_N when the spectral function of a hot fermion contains two peaks, separated by roughly the same energy as in the antiferromagnetically ordered state. This behavior has been obtained theoretically by departing from free fermions in a paramagnet and evaluating the dressed fermionic Green's function by summing up infinite series of noncrossed and crossed diagrams for the fermionic Green's function. The crossed diagrams describe vertex corrections. We show that keeping vertex corrections is crucial as the combined contribution from noncrossed diagrams broadens the spectral function of a hot fermion, but keeps its maximum at zero frequency. We argue, therefore, that to capture the physics of a magnetic pseudogap, one has to go beyond self-consistent one-loop theories, such as, e.g., Eliashberg theory for superconductivity. This result is relevant for the understanding of the observed reduction of superconducting T_c when superconductivity comes out of a pseudogap phase as within the Eliashberg theory thermal fluctuations do not affect T_c. We expect that similar results hold for incommensurate spin fluctuations.

We also analyzed the potential pseudogap behavior at $T = 0$ due to quantum fluctuations, assuming no superconductivity. We found that pseudogap may exist at a finite correlation length ξ and may even extend into the strong coupling regime. Still, this pseudogap behavior is not the precursor to the ordered state but rather the consequence of the fact that when spin fluctuations are weakly damped propagating massive bosons, the spectral function of a hot fermion is strongly reduced below the threshold set by the bosonic mass. We found that sufficiently close to an antiferromagnetic QCP, the spectral function of a hot fermion does not display pseudogap behavior at $T = 0$. Combining this with the result of our earlier work [30] that thermal fluctuations do not give rise to pseudogap behavior when the ground state is not ordered, we conclude that when the ground state is not magnetically ordered, there is no magnetic pseudogap at any T due to long-range magnetic fluctuations. A potential pseudogap due to short-range fluctuations in a doped Mott insulator has been analyzed in Ref. [54].

Acknowledgments. We thank Leon Balents, Erez Berg, Rafael Fernandes, Antoine Georges, Patrick Lee, Izabella Lovas, Michael Sadovskii, Subir Sachdev, Jörg Schmalian, Fedor Simkovic, and particularly André-Marie Tremblay for helpful discussions and suggestions. M.Y. was supported by the Gordon and Betty Moore Foundation through Grant No. GBMF8690 to UCSB by a grant from the Simons Foundation (Grant No. 216179, LB), and by the National Science Foundation under Grant No. NSF PHY-1748958. A.V.C. was supported by the U.S. Department of Energy, Office of Science, Basic Energy Sciences, under Award No. DE-SC0014402.

[1] M. A. Metlitski and S. Sachdev, Quantum phase transitions of metals in two spatial dimensions. II. Spin density wave order, Phys. Rev. B **82**, 075128 (2010).

[2] Y. Wang and A. Chubukov, Charge-density-wave order with momentum $(2q, 0)$ and $(0, 2q)$ within the spin-fermion model: Continuous and discrete symmetry breaking, preemptive composite order, and relation to pseudogap in hole-doped cuprates, Phys. Rev. B **90**, 035149 (2014).

[3] D. Chowdhury and S. Sachdev, Feedback of superconducting fluctuations on charge order in the underdoped cuprates, Phys. Rev. B **90**, 134516 (2014).

[4] W. A. Atkinson, A. P. Kampf, and S. Bulut, Charge order in the pseudogap phase of cuprate superconductors, New J. Phys. **17**, 013025 (2015).

[5] R. Arpaia, S. Caprara, R. Fumagalli, G. D. Vecchi, Y. Y. Peng, E. Andersson, D. Betto, G. M. D. Luca, N. B. Brookes, F. Lombardi, M. Salluzzo, L. Braicovich, C. D. Castro, M. Grilli, and G. Ghiringhelli, Dynamical charge density fluctuations pervading the phase diagram of a Cu-based high-T_c superconductor, Science **365**, 906 (2019).

[6] C. M. Varma, Non-fermi-liquid states and pairing instability of a general model of copper oxide metals, Phys. Rev. B **55**, 14554 (1997).

[7] C. M. Varma, Pseudogap Phase and the Quantum-Critical Point in Copper-Oxide Metals, Phys. Rev. Lett. **83**, 3538 (1999).

[8] S. Sachdev, H. D. Scammell, M. S. Scheurer, and G. Tarnopolsky, Gauge theory for the cuprates near optimal doping, Phys. Rev. B **99**, 054516 (2019).

[9] Y.-H. Zhang and S. Sachdev, From the pseudogap metal to the fermi liquid using ancilla qubits, Phys. Rev. Res. **2**, 023172 (2020).

[10] E. Mascot, A. Nikolaenko, M. Tikhanovskaya, Y.-H. Zhang, D. K. Morr, and S. Sachdev, Electronic spectra with paramagnon fractionalization in the single-band Hubbard model, Phys. Rev. B **105**, 075146 (2022).

[11] A. Nikolaenko, J. von Milczewski, D. G. Joshi, and S. Sachdev, Spin density wave, Fermi liquid, and fractionalized phases in a theory of antiferromagnetic metals using paramagnons and bosonic spinons, Phys. Rev. B **108**, 045123 (2023).

[12] M. Christos, Z.-X. Luo, H. Shackleton, Y.-H. Zhang, M. S. Scheurer, and S. Sachdev, A model of d-wave superconductivity, antiferromagnetism, and charge order on the square lattice, Proc. Natl. Acad. Sci. USA **120**, e2302701120 (2023).

[13] Y. M. Vilk and A. M. S. Tremblay, Destruction of fermi-liquid quasiparticles in two dimensions by critical fluctuations, Europhys. Lett. **33**, 159 (1996).

[14] Y. M. Vilk and A.-M. S. Tremblay, Non-perturbative many-body approach to the Hubbard model and single-particle pseudogap, J. Phys. I **7**, 1309 (1997).
[15] J. Schmalian, D. Pines, and B. Stojković, Weak Pseudogap Behavior in the Underdoped Cuprate Superconductors, Phys. Rev. Lett. **80**, 3839 (1998).
[16] J. Schmalian, D. Pines, and B. Stojković, Microscopic theory of weak pseudogap behavior in the underdoped cuprate superconductors: General theory and quasiparticle properties, Phys. Rev. B **60**, 667 (1999).
[17] É. Z. Kuchinskii and M. V. Sadovskii, Models of the pseudogap state of two-dimensional systems, J. Exp. Theor. Phys. **88**, 968 (1999).
[18] C. P. Moca, I. Tifrea, and M. Crisan, An analytical approach for the pseudogap in the spin fluctuations model, J. Supercond. **13**, 411 (2000).
[19] M. V. Sadovskii, Pseudogap in high-temperature superconductors, Phys.-Usp. **44**, 515 (2001).
[20] Y. Yanase, Pseudogap and superconducting fluctuation in high-tc cuprates: Theory beyond 1-loop approximation, J. Phys. Soc. Jpn. **73**, 1000 (2004).
[21] S. Roy and A.-M. S. Tremblay, Scaling and commensurate-incommensurate crossover for the d=2, z=2 quantum critical point of itinerant antiferromagnets, Europhys. Lett. **84**, 37013 (2008).
[22] T. A. Sedrakyan and A. V. Chubukov, Pseudogap in underdoped cuprates and spin-density-wave fluctuations, Phys. Rev. B **81**, 174536 (2010).
[23] J. P. F. LeBlanc, A. E. Antipov, F. Becca, I. W. Bulik, G. K.-L. Chan, C.-M. Chung, Y. Deng, M. Ferrero, T. M. Henderson, C. A. Jiménez-Hoyos, E. Kozik, X.-W. Liu, A. J. Millis, N. V. Prokof'ev, M. Qin, G. E. Scuseria, H. Shi, B. V. Svistunov, L. F. Tocchio, I. S. Tupitsyn *et al.* (Simons Collaboration on the Many-Electron Problem), Solutions of the Two-Dimensional Hubbard Model: Benchmarks and Results from a Wide Range of Numerical Algorithms, Phys. Rev. X **5**, 041041 (2015).
[24] O. Gunnarsson, T. Schäfer, J. P. F. LeBlanc, E. Gull, J. Merino, G. Sangiovanni, G. Rohringer, and A. Toschi, Fluctuation Diagnostics of the Electron Self-Energy: Origin of the Pseudogap Physics, Phys. Rev. Lett. **114**, 236402 (2015).
[25] M. Ye and A. V. Chubukov, Hubbard model on a triangular lattice: Pseudogap due to spin density wave fluctuations, Phys. Rev. B **100**, 035135 (2019).
[26] T. Schäfer, N. Wentzell, F. Šimkovic, Y.-Y. He, C. Hille, M. Klett, C. J. Eckhardt, B. Arzhang, V. Harkov, F. m. c.-M. Le Régent, A. Kirsch, Y. Wang, A. J. Kim, E. Kozik, E. A. Stepanov, A. Kauch, S. Andergassen, P. Hansmann, D. Rohe, Y. M. Vilk *et al.*, Tracking the Footprints of Spin Fluctuations: A MultiMethod, MultiMessenger Study of the Two-Dimensional Hubbard Model, Phys. Rev. X **11**, 011058 (2021).
[27] K. Held, Beyond DMFT: Spin fluctuations, pseudogaps and superconductivity, *Dynamical Mean-Field Theory of Correlated Electrons*, edited by E. Pavarini, E. Koch, A. Lichtenstein, and D. Vollhardt, Modeling and Simulation Vol. 12 (Forschungszentrum Jülich GmbH Zentralbibliothek, Verlag, Germany, 2022).
[28] F. Krien, P. Worm, P. Chalupa, A. Toschi, and K. Held, Explaining the pseudogap through damping and antidamping on the Fermi surface by imaginary spin scattering, Commun. Phys. **5**, 336 (2022).
[29] F. Šimkovic IV, R. Rossi, and M. Ferrero, Two-dimensional Hubbard model at finite temperature: Weak, strong, and long correlation regimes, Phys. Rev. Res. **4**, 043201 (2022); F. Simkovic, R. Rossi, A. Georges, and M. Ferrero, Origin and fate of the pseudogap in the doped Hubbard model, arXiv:2209.09237.
[30] M. Ye, Z. Wang, R. M. Fernandes, and A. V. Chubukov, Location and thermal evolution of the pseudogap due to spin fluctuations, arXiv:2304.08623.
[31] M. R. Norman, M. Randeria, H. Ding, and J. C. Campuzano, Phenomenology of the low-energy spectral function in high-T_c superconductors, Phys. Rev. B **57**, R11093 (1998).
[32] M. Franz and A. J. Millis, Phase fluctuations and spectral properties of underdoped cuprates, Phys. Rev. B **58**, 14572 (1998).
[33] S. Fujimoto, Pseudogap phenomena in the BCS pairing model, J. Phys. Soc. Jpn. **71**, 1230 (2002).
[34] E. Berg and E. Altman, Evolution of the Fermi Surface of d-Wave Superconductors in the Presence of Thermal Phase Fluctuations, Phys. Rev. Lett. **99**, 247001 (2007).
[35] Y.-M. Wu, S.-S. Zhang, A. Abanov, and A. V. Chubukov, Interplay between superconductivity and non-Fermi liquid behavior at a quantum-critical point in a metal. V. The γ model and its phase diagram: The case $\gamma = 2$, Phys. Rev. B **103**, 184508 (2021).
[36] Z. Dai and P. A. Lee, Superconductinglike response in a driven gapped bosonic system, Phys. Rev. B **104**, 054512 (2021).
[37] X.-C. Wang and Y. Qi, Phase fluctuations in two-dimensional superconductors and pseudogap phenomenon, Phys. Rev. B **107**, 224502 (2023).
[38] Z. Dai, T. Senthil, and P. A. Lee, Modeling the pseudogap metallic state in cuprates: Quantum disordered pair density wave, Phys. Rev. B **101**, 064502 (2020).
[39] O. Grossman and E. Berg, Weakly damped bosons and precursor gap in the vicinity of an antiferromagnetic metallic transition, arXiv:2304.12697.
[40] See Supplemental Material at http://link.aps.org/supplemental/10.1103/PhysRevB.108.L081118 for more details of the (1) self-consistent one loop theory; (2) toy models for the pseudogap behavior; and (3) pseudogap at $T = 0$.
[41] We note in passing that the total spectral weight is the same as in $A^{(1)}(\mathbf{k}_{\rm hs}, \bar{\omega})$ where at such $\lambda_{\rm th}$ it is concentrated around the near-δ-functional peaks at $|\bar{\omega}| = \tilde{\Delta}_{\rm pg}$.
[42] M. V. Sadovskiĭ, A model of a disordered system (A contribution to the theory of "liquid semiconductors"), Sov. J. Exp. Theor. Phys. **39**, 845 (1974); Theory of quasi-one-dimensional systems undergoing peierls transition, Sov. Phys. Solid State **16**, 1632 (1974); Exact solution for the density of electronic states in a model of a disordered system, Zh. Eksp. Theor. Fiz. **77**, 2070 (1979) [Sov. Phys. JETP **50**, 989 (1979)]; M. V. Sadovskii, *Diagrammatics: Lectures on Selected Problems in Condensed Matter Theory* (World Scientific, Singapore, 2006).
[43] We note in passing that within SCOLT, the Green's function can also be represented as an infinite sum of multiloop diagrams, such as in Eq. (4) but with the combinatoric factor $\mathcal{D}_m = 2^{2m+1}(2m-1)!!/(2m+2)!!$. Solving Eq. (4) with this $\mathcal{D}_m$, we reproduce the spectral function solution of $A^{(\rm sc)}(\mathbf{k}_{\rm hs}, \bar{\omega}) \propto \sqrt{4\tilde{\Delta}_{\rm pg}^2 - \bar{\omega}^2}$.

[44] Y. Gu, A. Kitaev, S. Sachdev, and G. Tarnopolsky, Notes on the complex sachdev-ye-kitaev model, J. High Energy Phys. 02 (2020) 157.
[45] A. Georges, O. Parcollet, and S. Sachdev, Quantum fluctuations of a nearly critical Heisenberg spin glass, Phys. Rev. B **63**, 134406 (2001).
[46] Y. Wang and A. V. Chubukov, Quantum phase transition in the Yukawa-SYK model, Phys. Rev. Res. **2**, 033084 (2020).
[47] A finite negative $\delta\mu$ relates the observable photoemission intensity $I(\mathbf{k}_{\rm hs},\omega) = A^{\rm full}(\mathbf{k}_{\rm hs},\omega)n_F(\omega)$ to the behavior of $A^{\rm full}(\mathbf{k}_{\rm hs},\bar{\omega})$ at negative $\bar{\omega}$, subject to $\bar{\omega} < -|\delta\mu|$. Because of this constraint, the singular behavior of $\Sigma_{\rm th}(z)$ and $\Gamma(z)$ at $z \to 0$ [Fig. 4(d)] is not accessible in photoemission experiments.
[48] E. G. C. P. van Loon, F. Krien, H. Hafermann, A. I. Lichtenstein, and M. I. Katsnelson, Fermion-boson vertex within dynamical mean-field theory, Phys. Rev. B **98**, 205148 (2018).
[49] A. I. Posazhennikova and M. V. Sadovskii, The Ginzburg-Landau expansion in the simple model of a superconductor with a pseudogap, J. Exp. Theor. Phys. **88**, 347 (1999).
[50] E. Z. Kuchinskii and M. V. Sadovskii, Superconductivity in a simple model of the pseudogap state, J. Exp. Theor. Phys. **90**, 535 (2000).
[51] A. Abanov, A. V. Chubukov, and J. Schmalian, Quantum-critical theory of the spin-fermion model and its application to cuprates: Normal state analysis, Adv. Phys. **52**, 119 (2003).
[52] This δ function is obtained by either adding $i0$ to ω [this corresponds to treating $T = 0$ as the limit $T \to 0$ and using the fact that at any finite T, Im $\Sigma(\mathbf{k}, 0)$ is finite], or by evaluating $A^{\rm q}(\mathbf{k},\omega)$ at $\mathbf{k}$ for which $\epsilon_{\mathbf{k}+\mathbf{Q}}$ is finite, and taking the limit $\mathbf{k} \to \mathbf{k}_{\rm hs}$.
[53] In principle, there may be another possibility to suppress the Landau damping even without requiring $v_s \ll v_F$. Namely, if one *assumes* that the pseudogap exists and evaluates γ using the Green's functions with the pseudogap, one finds that γ indeed gets reduced. We do not know, however, whether such a state can be ever reached by approaching a QCP from the paramagnetic state.
[54] D. Sénéchal and A.-M. S. Tremblay, Hot Spots and Pseudogaps for Hole- and Electron-Doped High-Temperature Superconductors, Phys. Rev. Lett. **92**, 126401 (2004).